Accepted Manuscript

Integrated electrochemical analysis of polyvinyl pyrrolidone (PVP) as the inhibitor for copper chemical mechanical planarization (Cu-CMP)

Guang Yang, Haixu Wang, Ning Wang, Rong Sun, Ching-Ping Wong

PII: S0925-8388(18)32974-8

DOI: 10.1016/j.jallcom.2018.08.101

Reference: JALCOM 47189

To appear in: *Journal of Alloys and Compounds*

Received Date: 31 March 2018

Revised Date: 29 July 2018

Accepted Date: 11 August 2018

Please cite this article as: G. Yang, H. Wang, N. Wang, R. Sun, C.-P. Wong, Integrated electrochemical analysis of polyvinyl pyrrolidone (PVP) as the inhibitor for copper chemical mechanical planarization (Cu-CMP), *Journal of Alloys and Compounds* (2018), doi: 10.1016/j.jallcom.2018.08.101.

Integrated electrochemical analysis of polyvinyl pyrrolidone (PVP) as the inhibitor for copper chemical mechanical planarization (Cu-CMP)

Guang Yang[a, b], Haixu Wang[a, c], Ning Wang[a*], Rong Sun[a, e*], and Ching-Ping Wong [a, d]

[a] Shenzhen Institutes of advanced technology, Chinese academy of sciences, Shenzhen 518055, P.R. China

[b] Department of Nano Science and Technology Institute, University of Science and Technology of China, Suzhou 215123, China

[c] College of Materials Science and Engineering, Shenzhen University, Shenzhen 518060, China

[d] Department of Electronics Engineering, The Chinese University of Hong Kong, Hong Kong 999077, China

[e] Guangdong Provincial Key Laboratory of Materials for High Density Electronic Packaging, Shenzhen Institutes of Advanced Technology, Chinese Academy of Sciences, Shenzhen 518055, China

[*] Corresponding author. Email: ning.wang@siat.ac.cn (WN); rong.sun@siat.ac.cn (SR)

Abstract. Copper chemical mechanical planarization (Cu-CMP) is an essential procedure for the fabrication of integrated circuits (IC). The corrosion inhibitors in the Cu-CMP slurry could balance the over etching from the corrosion reagents to facilitate the global planarization of the copper layers. However, the normally used Cu-CMP inhibitor 1-benzotriazole (BTA) was toxic for the long time usage. In this paper, the biocompatible polyvinyl pyrrolidone (PVP) was proposed to substitute the BTA in the Cu-CMP. With an integrated electrochemical test, including the Tafel polarization, electrochemical impedance spectra (EIS), and the electrochemical noise (EN), it was found that the PVP could possess a good inhibition effect comparable to BTA, which opened up a promising way for the design of biocompatible inhibitors in the Cu-CMP.

Keywords: Chemical mechanical planarization; Electrochemical impedance spectra; Electrochemical noise; Slurry; Inhibitors

1. Introduction

As an emerging technology, the three dimensional (3D) electronic packaging based on the through silicon via (TSV) has been utilized to fabricate the ultra-large scale integration circuits (ULSI) [1-5]. In order to improve the yield of TSV, the chemical mechanical planarization (CMP) has been applied to remove and polish the excess electroplated copper layer using the Cu-CMP slurry. The global planarization of the copper layer in the Cu-CMP process was achieved via the synergistic effect between the chemical corrosion and the mechanical abrasion [6-8]. The typical Cu-CMP slurry is composed of oxidizer, coordination/chelation agents, corrosion inhibitors, surfactants, and the metal oxide abrasives (eg., Al_2O_3 and SiO_2), where the chemical components and the abrasives were used for chemical corrosion and the mechanical abrasion, respectively [9-13].

In the Cu-CMP slurry, the oxidizer was used to oxidize the copper layer to generate a soft and active $CuO/Cu(OH)_2/Cu_2O$ film on the surface that facilitated the material removing [10, 14, 15]. The inhibitor was used to balance the over etching and protect the concave positions on the copper surface that was critical for the global planarization [16-19]. With respect to the chelating agents, they were developed to etch the copper layer via coordinating with the oxidized $CuO/Cu(OH)_2/Cu_2O$ on the copper surface [12, 20, 21].

In order to optimize the planarization effect of the Cu-CMP slurry, the electrochemical methods have been widely used to investigate the behaviors of the chemical components. As reported in literatures, *Tafel* polarization was used to determine the corrosion potential and the corrosion current under different chelating agents and corrosion inhibitors [11, 13, 17, 22, 23]. The electrochemical impedance spectra (EIS) was used to determine the solution/charge transfer resistance as well as the double layer capacitance [15, 19, 24-26]. Both of *Tafel* polarization and EIS have been regarded as the powerful technique to investigate the material removing and planarization mechanism of the Cu-CMP slurries. In addition, the electrochemical noise (EN) could also be utilized to analyze the Cu-CMP process, especially for the inhibition efficiency of the corrosion inhibitors [27-30]. However, the integrated electrochemical method, combining the *Tafel* polarization, EIS, static corrosion, and the EN has been rarely reported till now.

In the Cu-CMP slurry, the 1-benzotriazole (BTA) is the normally used corrosion inhibitor, which could be strongly absorbed on the copper surface and promote the global planarization [11]. However, the toxicity of BTA should be harmful to the health. Therefore, it is necessary to develop the low toxic or biocompatible inhibitors to substitute the BTA in the Cu-CMP slurry.

With this in mind, an integrated electrochemical method was presented to investigate the inhibition behaviors of the biocompatible polyvinyl pyrrolidone (PVP) for the copper layer, which was proposed to replace the BTA in the Cu-CMP slurry. The analysis revealed that the inhibition

effect of PVP for the copper layer could be comparable with that of BTA under the same condition.

2. Experimental section

All chemicals used in this paper, including the sodium hydroxide (NaOH, >97.0%, Aladdin Ltd.), potassium sorbate (>99.0%, Aladdin Ltd.), 1-benzotriazole (BTA, 99%, Aladdin Ltd.), polyvinyl pyrrolidone K-30 (PVP, AR, Ourchem Ltd.), ethylenediaminetetraacetic acid (EDTA, AR, 99.5%, Aladdin Ltd.), ethylenediaminetetraacetic acid disodium salt (EDTA-2Na, AR, ≥99.0%, Xilong Ltd.), glycine (Gly, AR, >99.5%, Sinopharm Ltd.), diethylenetriaminepentaacetic acid (DTPA, AR, >99.0%, Aladdin Ltd.), and nitrilotriacetic acid (NTA, >99.0%, Aladdin Ltd.) were used as received without any further purification.

2.1 Static corrosion

4 mg NaOH, 2 wt% H_2O_2, 0.5 wt% glycine and 150 ppm BTA/PVP were added into 100 mL deionized water under stirring to form the Cu-CMP slurry. A copper foil (99.9%) with an area 1×1 cm^2 was immersed in the slurry for 3-9 h at the room temperature. The weight loss was recorded in table S3-S5 and the average corrosion rate (mg/h) was calculated from 3 tests under the same condition.

2.2 Electrochemical studies

The electrochemical studies were performed based on the three-electrode system with an electrochemical workstation (CHI760E, Shanghai, China). The copper working electrode (99.9% copper rod in PTFE) was purchased from IDA Ltd. (Tianjin, China) with a surface area 7×10^{-2} cm^2. The copper electrode surface was firstly mirror-polished before the electrochemical measurement. The platinum electrode (IDA Ltd., Tianjin, China) with the surface area of 4 cm^2 was used as the counter electrode, and the Ag/AgCl electrode (IDA Ltd., Tianjin, China) was used

as the reference electrode. The slurry was prepared with 0.1 M NaOH, deionized water, chelating agent and corrosion inhibitors.

***Tafel polarization*.** To evaluate the behaviors of chelating agents and corrosion inhibitors, the three-electrode system was firstly immersed in the slurry for 15 min to get a stable open circuit potential (OCP), and then the *Tafel* polarization scanning was performed in a scan rate 5 mV/s at a voltage range around the OCP.

Electrochemical impedance spectra (EIS). In the EIS test, the three-electrode system was firstly immersed in the slurry for 0-120 min, and then the EIS scanning was carried out in a frequency range of 0.01-10^5 Hz for 800 s around the OCP. The EIS data were treated and fitted with the ZView software based on the single-layer and double-layer equivalent circuit modes for the inhibitor films [19].

Electrochemical noise (EN). In the EN test, the current and potential signals were collected with the Interval 0.1 s and the during time 2000 s. The analysis of EN data was performed in both time and frequency domains. In the time domain, the noise resistance R_n (the ratio between the standard deviation of potential and current noise) was collected for PVP (150 ppm) and BTA (150 ppm) based slurries.

The digital images for the copper surface before and after the static corrosion were recorded by a metallographic optical microscopy (LEICA DM 2700M), and the corresponding morphologies were determined with a field emission scanning electron microscopy (FESEM, Nova NanoSEM 450, FEI) at an accelerating voltage of 10 kV.

3. Results and discussion

3.1 Evaluating the inhibitors and chelating agents under *Tafel* polarization

Figure 1 showed the *Tafel* polarization curves of the copper electrode in 0.1 M NaOH solutions containing the BTA/PVP (50-200 ppm) inhibitors. The corrosion potential E_{corr} and corrosion

current density j_{corr} were calculated from Figure 1. As shown in Figure 1A, with increasing the BTA concentration from 50 to 200 ppm, the corrosion potential E_{corr} was positively changed from -182 to -142 mV, and the corrosion current density j_{corr} was gradually deceased from 54.0 to 3.4 μA cm^{-2}, suggesting the outstanding inhibition effect of BTA, which was consistent with the investigations in literatures [21, 31]. Comparatively, with increasing the PVP concentration from 50 to 200 ppm, the E_{corr} was slightly changed from -180 to -184 mV, and the j_{corr} was changed from 33.0 to 54.2 μA cm^{-2} (Figure 1B), which was 38%-63% of the blank counterparts without any inhibitor, which indicated the effective inhibition of PVP. The strong inhibition of BTA for the copper should be ascribed to the coordination bonding of BTA molecules to the copper surface with one or two nitrogen donors [32], and the relatively weak inhibition effect of PVP should be owing to the less coordination sites (only one oxygen donor) and the strong steric hindrance effect from the carbon chains (Figure 1D). The difference in molecular structure made BTA and PVP show different absorption modes on the copper surface, where Cu-BTA inhibition film should be absorbed on the copper surface with a mono-layer chemically absorption mode, while the Cu-PVP inhibition film should be absorbed on the copper surface with a double or multiple physically absorption mode. In addition, the potassium sorbate has also been evaluated as the inhibitor (see supporting information Figure S1, table S1), which gave a combination of E_{corr}= -50.4 mV and j_{corr}= 18.3 μA cm^{-2}, also indicating the good inhibition effect, in accordance with the literatures [16, 23, 33]. However, the K^+ form the potassium sorbate may result in serious ion pollution, which should give rise to the low yield for the IC fabrication. Therefore, it is meaningful to use PVP as an alternative biocompatible Cu-CMP inhibitor.

Regarding the effect of chelating agents, the slurry with the ligands EDTA (ethylenediaminetetraacetic acid)/ DTPA (diethylenetriaminepentaacetic acid)/ Gly (glycine)/ Na_2EDTA/ NTA (nitrilotriacetic acid) was tested in the *Tafel* polarization mode (Figure 1C) and

the corresponding E_{corr} and j_{corr} were tabulated in Table 2. As depicted in Figure 1C and table 2, Gly exhibited the largest j_{corr} (88.6 μA cm^{-2}) and a large negative E_{corr} (-208 mV), both of which indicated the best performance of Gly as the chelating agent in the slurry. Amongst the other chelating agents, the Na_2EDTA showed a most negative E_{corr} (-216 mV). However, the Na^+ cations may result in ion pollutions in the copper interconnects. In addition to the excellent chelating performance, Gly could also benefit the Cu-CMP with the low cost and low toxicity. Therefore, in the Cu-CMP slurries, Gly could be a cost-effective and environmental friendly chelating agent. The open circuit potential (OCP) for the PVP and BTA (150 ppm) based slurries was measured as plots of potential versus time. As shown in Figure 1E and F, a stable OCP (-190/-160 mV) for the PVP/BTA based slurry could be reached after 900 s. The more positive OCP value for BTA could be due to its superior inhibition effect, which may also result in a lower material removing rate. Comparatively, the slightly negative OCP for PVP may supply a balance between the effective inhibition and the large material removing rate.

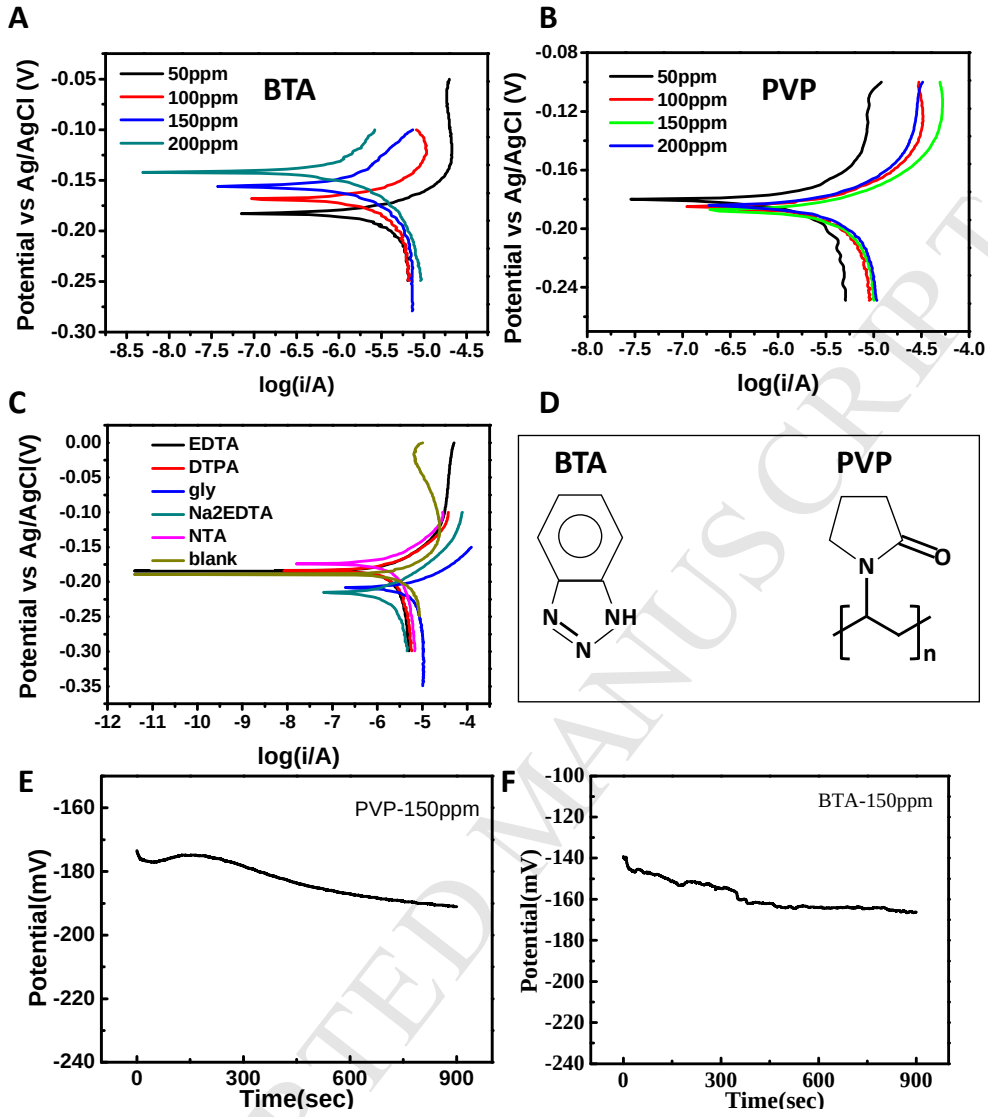

Figure 1. A) Potentiodynamic polarization curves for BTA based slurry under different BTA concentrations (50-200 ppm). B) Potentiodynamic polarization curves for PVP based slurry under different PVP concentrations (50-200 ppm). C) Potentiodynamic polarization curves for the inhibitor-free slurry with different chelating agents (EDTA/DTPA/Gly/Na_2EDTA/NTA). D) Molecular structures of the BTA and PVP molecules. The electrode area is 0.07 cm^2. (E) and (F) OCP test of the slurry containing PVP and BTA, respectively.

Table 1. E_{corr} and j_{corr} for PVP and BTA based alkaline slurries calculated from the potentiodynamic polarization curves.

Inhibitor	Concentration	E_{corr}/mV	j_{corr} [#] /μA cm^{-2}
blank	0	-189	86.7
PVP	50 ppm	-180	33.0
PVP	100 ppm	-185	41.0
PVP	150 ppm	-187	54.2
PVP	200 ppm	-184	54.2
BTA	50 ppm	-182	54.0
BTA	100 ppm	-168	33.5
BTA	150 ppm	-156	17.7
BTA	200 ppm	-142	3.4

[#] The electrode area is 0.07 cm^2. The derivate of the E_{corr}, j_{corr} is 10%.

Table2. E_{corr} and j_{corr} for inhibitor-free alkaline slurries with different chelating agents calculated from the potentiodynamic polarization curves.

Chelating agent	Concentration	E_{corr}/mV	j_{corr}/μA cm^{-2}
DTPA	0.5 wt%	-183	33.1
Na_2EDTA	0.5 wt%	-216	22.3
Gly	0.5 wt%	-208	88.6
EDTA	0.5 wt%	-183	35.4

NTA	0.5 wt%	-174	20.3

Note. The derivate of the E_{corr}, j_{corr} is 10%.

3.2 Static corrosion

In order to predict the corrosion rate of the optimized alkaline slurry, the static corrosion was performed for the slurry composed of 4 mg NaOH, 2 wt% H_2O_2, 0.5 wt% Gly, and 150 ppm BTA/PVP. Before the corrosion test, the copper surface was mirror-polished firstly (Figure 2B), and then the copper plate was immersed in the alkaline slurries at room temperature for 3-9 hours. As shown in Figure 2A, after immersing in the alkaline slurry for 6 h, the material removal rate (dm/dt) could be calculated as the average weight loss rate from three parallel experiments (see supporting information, Table S3-S5). Without the activation by H_2O_2 (#4 slurry), the etching rate could be very low (0.08 mg/h), which was then highly improved to 0.29 mg/h after the addition of H_2O_2 (#1 slurry). With the addition of BTA, the etching rate could be reduced to 0.11 mg/h, which could be slightly increased to 0.16mg/h by replacing the BTA with PVP, indicating the similar inhibition performance for BTA and PVP. As shown in Figure 2C and 2D, in a millimeter-scale dimension, there was little difference after the static corrosion in the BTA and PVP based slurries. However, in a micro-scale dimension, a clear difference after the inhibition with BTA/PVP could be observed in Figure 2E and 2F. In comparison, a flat inhibition film could be found for the BTA based slurry, while a dense-packed needle like Cu-PVP inhibition film could be found for the PVP based slurry, which should be due to the different absorption modes of the inhibition films as described above. As shown in Figure 2G, the C, Cu, O-Kα elemental mapping also indicated the needle like morphology and the dense-packed nature of the Cu-PVP inhibition film on the copper surface.

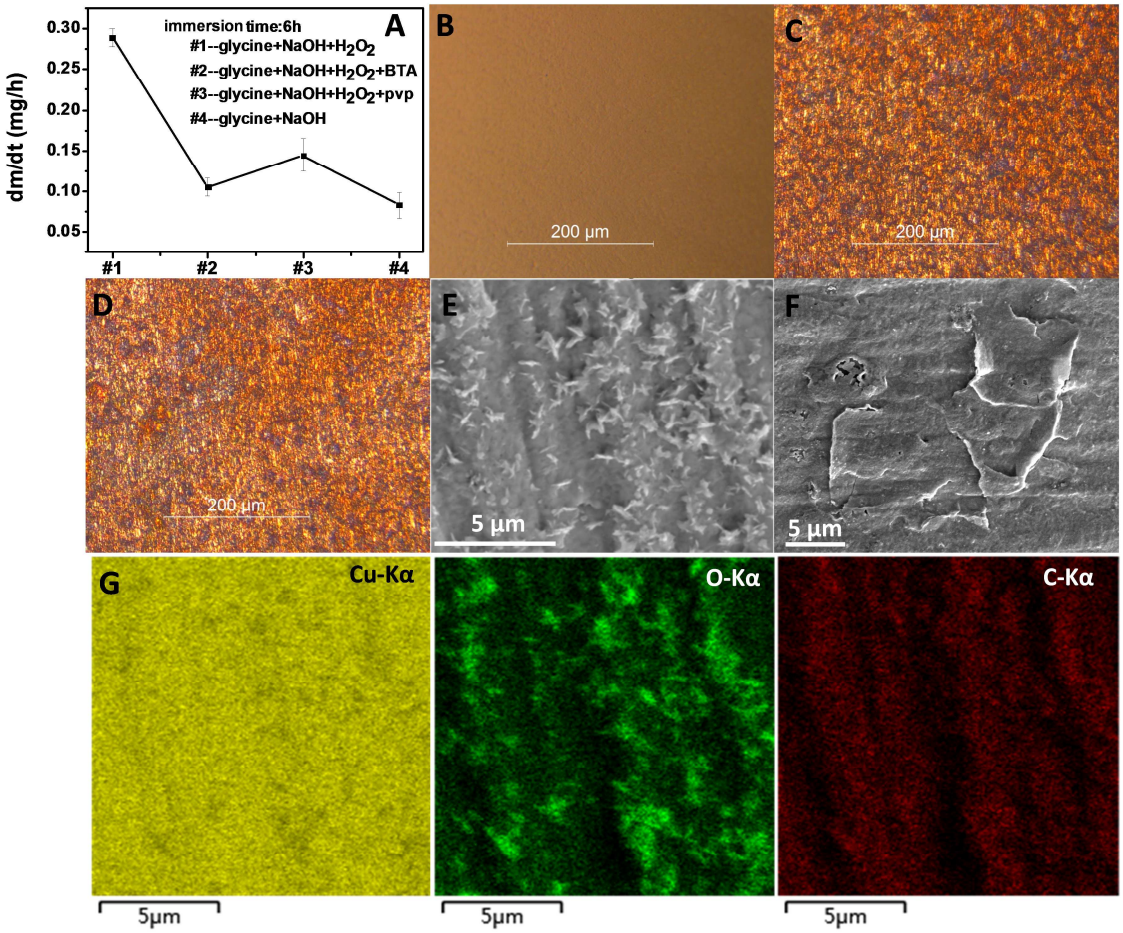

Figure 2. Static corrosion test. A) Corrosion rate under different slurries. B) Digital image of pristine polished copper surface. C) Digital image of the copper surface after immersing in #3 slurry for 6 h. D) Digital image of the copper surface after immersing in #2 slurry for 6 h. E) FESEM image of the copper surface after static corrosion in #3 slurry. F) FESEM image of the copper surface after static corrosion in #2 slurry. G) Corresponding Cu, O, C elemental mapping for the PVP absorbed Cu surface (E).

3.3 Electrochemcial impedance spectra

To further understand the different absorption modes of PVP and BTA molecules on the copper surface, the EIS characterization was performed for the PVP and BTA based slurries with the same concentration 150 ppm. The equivalent circuits (Figure 3A, 3B) were firstly established

based on modified modes for monolayer and double-layer absorption inhibition film [19]. In the equivalent circuits, C1, R1 and C2, R2 were the capacitance and resistance of the single-layer and double layer inhibition film, respectively. R_S was the solution resistance. W was the Warburg open Impedance for the linear part at low frequencies. C_{dl} was the double layer capacitance and R_{ct} was the charge transfer resistance. As shown in Figure 3C and 3D, after immersing in the BTA and PVP based slurries for 0-120 min, different Nyquist plots could be found, which should be owing to the coverage area evolution of the inhibition film and the film thickness. The Nyquist plots for BTA based slurry (Figure 3C) could be fitted well with the monolayer film mode (Figure 3A), which was in accordance with the chemical absorption mode of BTA molecules on the copper surface. Comparatively, for the EIS data of PVP based slurry (Figure 3D), only plots at t= 0 min could be fitted well with the monolayer film mode, and the other Nyquist plots over 30 min could only be fitted with the double layer film mode (Figure 3B), which was consistent with the physical absorption mode of PVP molecules on the copper surface. As shown in Table 3, the fitted C_1, R_1 for Cu-BTA film were 0.1-1.1 μF, 12.4-20.5 Ω and the fitted C_1/C_2, R_1/R_2 for Cu-PVP film (t= 30-120 min) were 6×10^{-8}-1.4 μF/0.1-30 μF and 8.1-12.2 Ω /3.8-7.6 Ω, respectively. The lower film resistance of Cu-PVP film should be due to the needle-like morphology as shown in Figure 2E, G and Figure S2 (see supporting information) that provided the effective inhibition and the decent material removing rate simultaneously. The Bode and the phase diagrams have been used to investigate the corrosion behavior of the slurries. As presented in Figure 3E, the slope of the linear part in the Bode diagram for the BTA slurry was -0.50 (30 min)/-0.38 (120 min), falling in the range from -0.2 to -0.5 for the equivalent circuit mode (Figure 3A), in consistent with the Nyquist fitting result. The larger impedance after increasing the immersion time from 30 to 120 min indicated the thicker film thickness of the Cu-BTA film that could effectively protect the copper surface from over corrosion. In the corresponding phase diagram,

the high frequency peak showed a shift to lower phase degree (50-35°) along with the increase of immersion time from 30 to 120 min, revealing the decline of impedance of the Cu-BTA film, which should be mainly due to the cracks on the Cu-BTA inhibition film as observed in Figure 2F. Comparatively, as to the PVP based slurry (Figure 3F), the phase degree for the high-frequency peaks in the phase diagram only showed slightly change ascribed to the little difference in the film thickness of Cu-PVP, but the high-frequency impedance in the Bode diagram showed an increase from 1.78 to 17.8 Ω at 100 MHz along with the immersion time, indicating the effective corrosion inhibition effect of PVP that was physically absorbed on the copper surface.

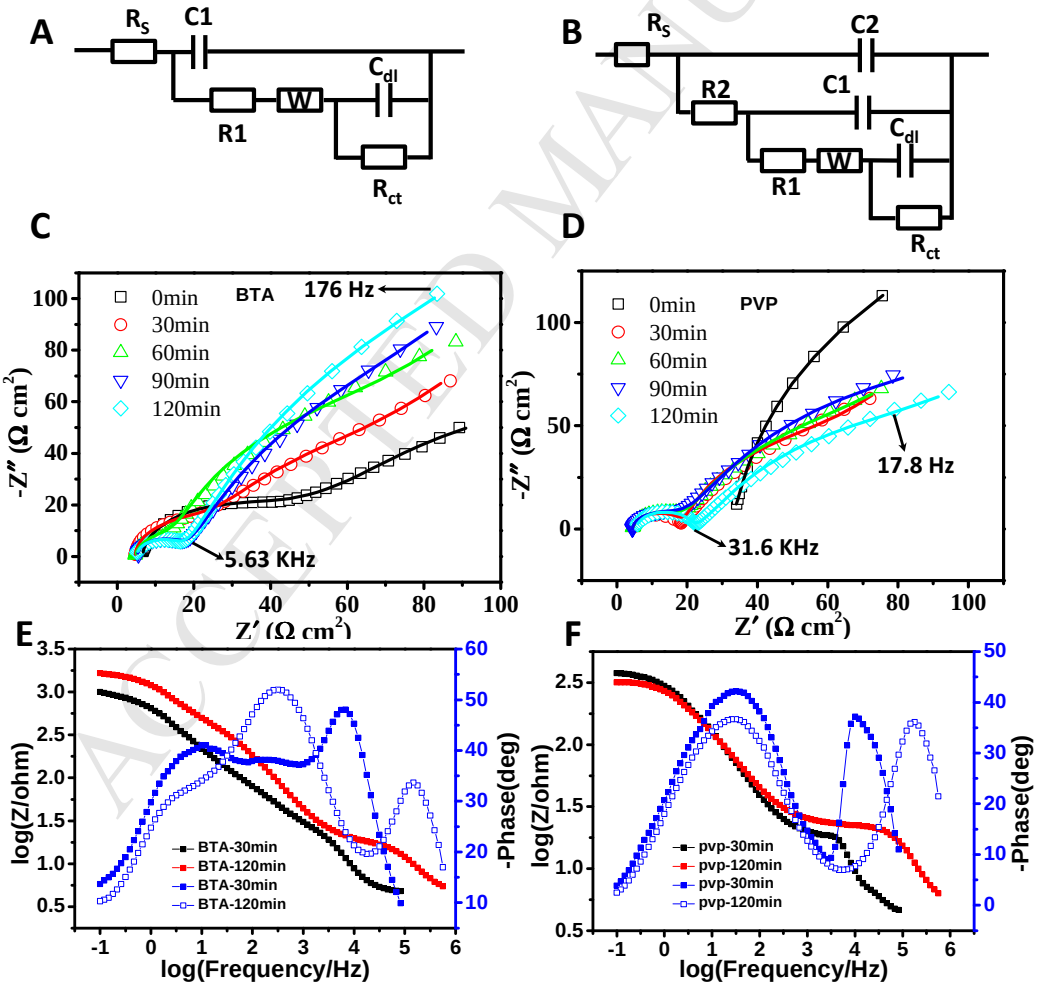

Figure 3. A) Equivalent circuit for single-layer inhibitor film. B) Equivalent circuit for double-layer inhibitor film. C1, R1 and C2, R2 are the capacitance and resistance for the single-layer and double layer inhibitor film, respectively. R_S is the solution resistance. W is the Warburg open Impedance. C_{dl} is the double layer capacitance and R_{ct} is the charge transfer resistance. C) and D) Nyquist plot under different immersion time (0-120 min) for BTA and PVP based slurries, respectively. Open dots and solid lines represent the experiment result and the best fitting result according to the equivalent circuits, respectively. E) and F) Bode and phase diagram for the BTA and PVP based slurries, respectively.

Table 3 EIS fitted parameters for the BTA and PVP based slurries containing Gly as chelating agents.

	BTA based slurry					PVP based slurry				
Time (min)	0	30	60	90	120	0	30	60	90	120
Mode	S	S	S	S	S	S	D	D	D	D
$R_s(\Omega)$	6.7	4.7	4.9	5.3	5.1	32.9	4.6	4.4	4.5	5.6
$C_1(\mu F)$	1.1	2.3	1.8	0.1	0.1	0.2	$6 \cdot 10^{-8}$	1.1	1.4	10^{-7}
$R_1(\Omega)$	20.5	24.4	14.9	12.7	12.4	92.8	10.2	10.5	8.1	12.2
$C_2(\mu F)$	N.A.	N.A.	N.A.	N.A.	N.A.	N.A.	1.6	2.5	3.0	0.1
$R_2(\Omega)$	N.A.	N.A.	N.A.	N.A.	N.A.	N.A.	4.5	4.6	7.6	3.8
$C_{dl}(\mu F)$	107	46.1	14.9	17.3	17.0	0.05	118	159	159	190
$R_{ct}(\Omega)$	42.0	19.6	44.8	32.1	50.5	204.3	34.0	30.2	31.8	28.9

Note: The mode 'S' and 'D' represent the single-layer and double-layer equivalent circuits, respectively. 'N.A.' means not applicable. The derivate of the fitted parameters is 10%.

3.4 Electrochemical noise

The potential and current noise data were recorded simultaneously to examine the corrosion behaviors of the alkaline slurries with BTA/PVP inhibitors. Figure 4 showed the potential and current noise for the BTA and PVP based slurries. As shown in Figure 4A, for the BTA based slurry, the voltage noise underwent a quick decline (< 500 s) and then a slow recovery while the current increased abruptly (< 500 s) and then fell slowly, which indicated the quick corrosion of the copper oxide film on the surface before 500s and the effective inhibition by BTA thereafter. In comparison, as to the PVP based slurry (Figure 4B), the corrosion was more moderate, which gave a chance for the balance between the effective inhibition and the large material removing rate.

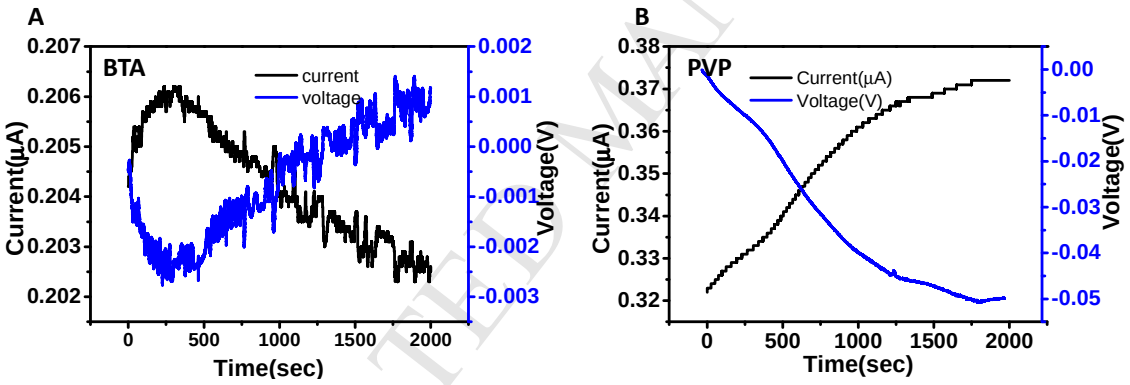

Figure 4. Pristine current and potential noise for BTA (A) and PVP (B) based slurries.

A polynomial fitting was used to treat the DC (direct current) trend removal of the current/potential noise [34]. After the treatment, the local corrosion information was attained as shown in Figure 5. In Figure 5A to 5D, zero current/voltage line represented the best fitting of the current and voltage noise, and the serrated peaks referred to the local corrosion. It was noticed that the current with PVP inhibitor vibrated in a range from -3 to 3 nA, while the current vibration range with BTA inhibitor was -1 to 1 nA, revealing the faster material removing rate under PVP than BTA.

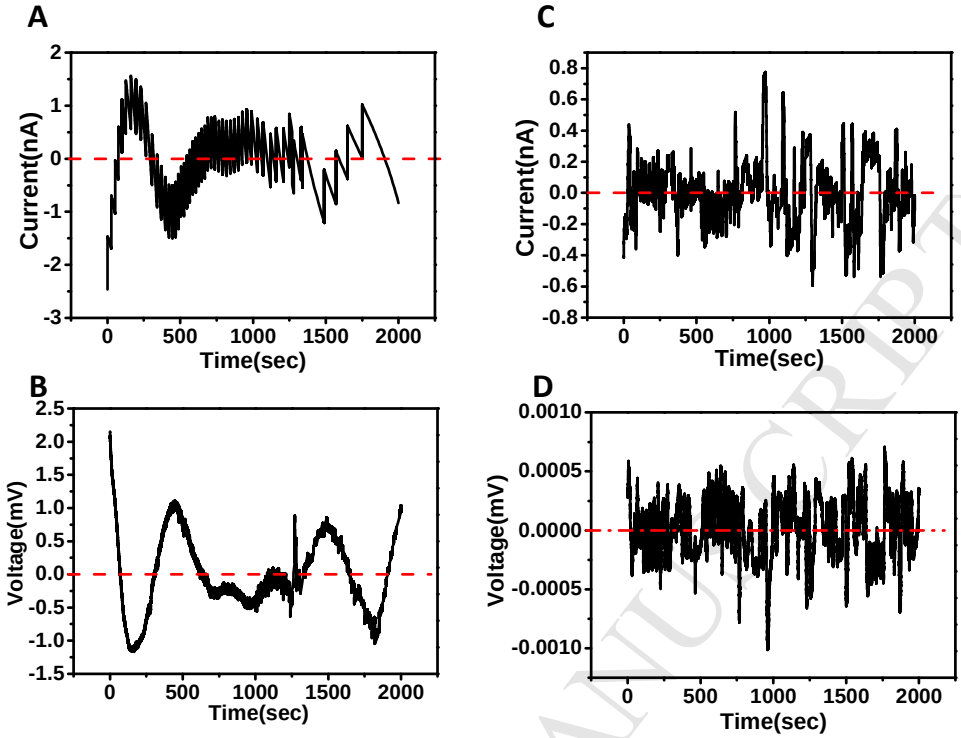

Figure 5. Current and potential noise data after DC trend removal for PVP (A, B) and BTA (C, D) based slurries.

Due to the strong correlation between the EN resistance R_n and the corrosion rate, R_n was determined from the time domain plots as the ratio of the standard deviation of potential noise $\boldsymbol{\sigma}_V$ over that of current noise $\boldsymbol{\sigma}_I$, ($R_n = \boldsymbol{\sigma}_V/\boldsymbol{\sigma}_I$). The calculated R_n was tabulated in Table 4, and was depicted in Figure 6. Along with the immersion time, the R_n for BTA and PVP based slurries could be in the range of 1250-1600 k Ω and 920-1000 k Ω, respectively. The larger R_n proved the better inhibition effect of the BTA molecules, and the similar R_n for the PVP also suggested a comparable inhibition effect.

After a Fast Fourier Transform (FFT), the time domain plots were transformed to the frequency domain plots (Figure 7). As shown in the PSD (power spectral density) plots, both PVP (Figure 7A) and BTA (Figure 7B) based slurries exhibited the relatively smooth curves with the slope from -1.8 to -1.1 dB/decade, which indicated the local corrosion behavior of the slurries.

Table 4. Standard deviation (σ) of potential, current noise and noise resistance R_n for PVP and BTA based slurries.

Immersion time(sec)	PVP based slurry			BTA based slurry		
	σ_V/v	σ_I/A	R_n/K Ω	σ_V/v	σ_I/A	R_n /K Ω
500	8.8×10^{-10}	8.7×10^{-4}	996	2.1×10^{-4}	1.4×10^{-10}	1509
1000	6.9×10^{-10}	6.7×10^{-4}	961	2.5×10^{-4}	1.8×10^{-10}	1417
1500	6.3×10^{-10}	5.8×10^{-4}	923	2.5×10^{-4}	1.9×10^{-10}	1285
2000	6.0×10^{-10}	5.7×10^{-4}	955	2.6×10^{-4}	2.1×10^{-10}	1259

Note. The derivate of the parameters is 10%.

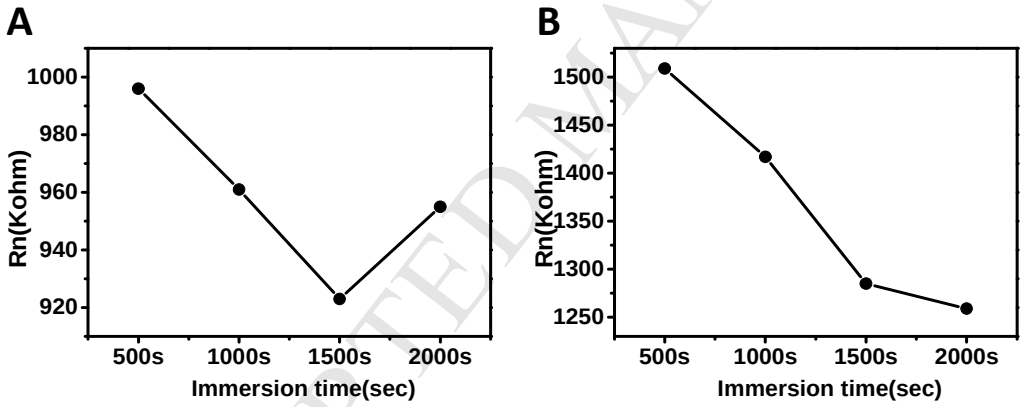

Figure 6. Noise resistance (R_n) for PVP (A) and BTA (B) based slurries.

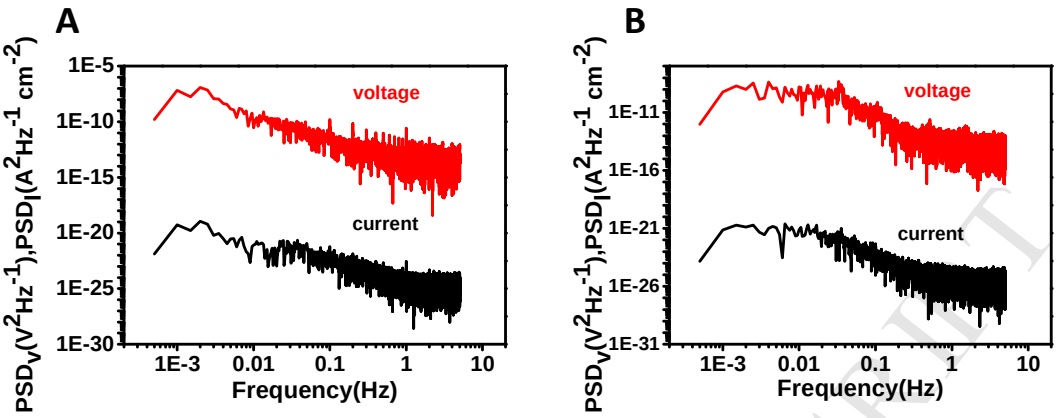

Figure 7. Frequency domain PSD plots for PVP (A) and BTA (B) based slurries.

4. Conclusions

In summary, a new PVP-based Cu-CMP slurry was proposed and analyzed by an integrated electrochemical method, where the *Tafel* polarization, EIS, and EN were simultaneously utilized to analyze the inhibition behaviors of PVP for the copper layer that has not been reported. The analysis revealed that the PVP inhibitor could exhibit the comparable inhibition effect compared with the BTA normally used in the Cu-CMP, which provided an alternative corrosion inhibitor for the copper layer removal and planarization. Moreover, the low cost and the biocompatibility of PVP also make it a promising environment friendly inhibitor for the scale-up fabrication. In the near future, the optimization of PVP inhibitor will be completed for the real Cu-CMP applications.

Acknowledgments

This work was supported by the National Key R&D Project from Minister of Science and Technology of China (2017YFB0406200）， National and Local Joint Engineering Laboratory of Advanced Electronic Packaging Materials（Shenzhen Development and Reform Committee 2017-934）, Leading Scientific Research Project of Chinese Academy of Sciences (QYZDY-SSW-JSC010), Guangdong Provincial Key Laboratory (2014B030301014), and R&D Funds for basic Research Program of Shenzhen (Grant No. JCYJ20160331191741738, JSGG20160229194437896).

References

[1] D. Lu, C.P. Wong, Materials for Advanced Packaging, 2 ed., Springer US, Boston, MA, 2009.

[2] J. Kim, J.S. Pak, J. Cho, E. Song, J. Cho, H. Kim, T. Song, J. Lee, H. Lee, K. Park, High-Frequency Scalable Electrical Model and Analysis of a Through Silicon Via (TSV), IEEE Transactions on Components Packaging & Manufacturing Technology, 1 (2011) 181-195.

[3] G. Katti, M. Stucchi, K.D. Meyer, W. Dehaene, Electrical Modeling and Characterization of Through Silicon via for Three-Dimensional ICs, IEEE Transactions on Electron Devices, 57 (2010) 256-262.

[4] C.S. Selvanayagam, J.H. Lau, X. Zhang, S.K.W. Seah, K. Vaidyanathan, T.C. Chai, Nonlinear Thermal Stress/Strain Analyses of Copper Filled TSV (Through Silicon Via) and Their Flip-Chip Microbumps, IEEE Transactions on Advanced Packaging, 32 (2009) 720-728.

[5] U. Kang, H.-J. Chung, S. Heo, D.-H. Park, H. Lee, J.H. Kim, S.-H. Ahn, S.-H. Cha, J. Ahn, D. Kwon, 8 Gb 3-D DDR3 DRAM Using Through-Silicon-Via Technology, IEEE Journal of Solid-State Circuits, 45 (2009) 111-119.

[6] G. Pan, N. Wang, H. Gong, Y. Liu, An empirical approach to explain the material removal rate for copper chemical mechanical polishing, Tribol. Int., 47 (2012) 142-144.

[7] D. Zhan, L. Han, J. Zhang, Q. He, Z.-W. Tian, Z.-Q. Tian, Electrochemical micro/nano-machining: principles and practices, Chem. Soc. Rev., 46 (2017) 1526-1544.

[8] A.E.K. Mohammad, D. Wang, Electrochemical mechanical polishing technology: recent developments and future research and industrial needs, The International Journal of Advanced Manufacturing Technology, 86 (2016) 1909-1924.

[9] N. Wang, G. Pan, Y. Liu, Synergistic roles of mixed inhibitors and the application of mixed complexing ligands in copper chemical mechanical polishing, Microelectron. Eng., 88 (2011) 3372-3374.

[10] D. Lee, H. Lee, H. Jeong, Slurry Components in Metal Chemical Mechanical Planarization (CMP) Process: Review, Int. J. Precis. Eng. Manuf., 17 (2016) 1751-1762.

[11] G. Tansuğ, T. Tüken, E.S. Giray, G. Fındıkkıran, G. Sığırcık, O. Demirkol, M. Erbil, A new corrosion inhibitor for copper protection, Corros. Sci., 84 (2014) 21-29.

[12] E. Matijevic, S.V. Babu, Colloid aspects of chemical-mechanical planarization, J. Colloid Interface Sci., 320 (2008) 219-237.

[13] P.B. Zantye, A. Kumar, A.K. Sikder, Chemical mechanical planarization for microelectronics applications, Mater. Sci. Eng. R-Rep., 45 (2004) 89-220.

[14] C. Yao, X. Niu, C. Wang, Y. Liu, Z. Jiang, Y. Wang, S. Tian, Study on the Weakly Alkaline Slurry of Copper Chemical Mechanical Planarization for GLSI, ECS Journal of Solid State Science and Technology, 6 (2017) P499-P506.

[15] T. Du, A. Vijayakumar, V. Desai, Effect of hydrogen peroxide on oxidation of copper in CMP slurries containing glycine and Cu ions, Electrochim. Acta, 49 (2004) 4505-4512.

[16] M. Nagar, J. Vaes, Y. Ein-Eli, Potassium sorbate as an inhibitor in copper chemical mechanical planarization slurries. Part II: Effects of sorbate on chemical mechanical planarization performance, Electrochim. Acta, 55 (2010) 2810-2816.

[17] Y. Ein-Eli, D. Starosvetsky, Review on copper chemical–mechanical polishing (CMP) and post-CMP cleaning in ultra large system integrated (ULSI)—An electrochemical perspective, Electrochim. Acta, 52 (2007) 1825-1838.

[18] A.B. Samui, J.G. Chavan, V.R. Hande, Study on film forming organo-copper polymer, Prog. Org. Coat., 57 (2006) 301-306.

[19] Y.J. Tan, S. Bailey, B. Kinsella, An investigation of the formation and destruction of corrosion inhibitor films using electrochemical impedance spectroscopy (EIS), Corros. Sci., 38 (1996) 1545-1561.

[20] M.C. Bernard, C. Gabrielli, S. Joiret, C. Mace, E. Ostermann, A. Pailleret, Investigations on the corrosion of copper patterns in the course of the "post-CMP cleaning" of integrated electronic microcircuits in oxalic acid aqueous solutions, Electrochim. Acta, 53 (2007) 1325-1335.

[21] C. Yan, Y. Liu, J. Zhang, C. Wang, W. Zhang, P. He, G. Pan, Synergistic Effect of Glycine and BTA on Step Height Reduction Efficiency after Copper CMP in Weakly Alkaline Slurry, ECS Journal of Solid State Science and Technology, 6 (2017) P1-P6.

[22] K.G. Shattuck, J.-Y. Lin, P. Cojocaru, A.C. West, Characterization of phosphate electrolytes for use in Cu electrochemical mechanical planarization, Electrochim. Acta, 53 (2008) 8211-8216.

[23] Y.N. Prasad, S. Ramanathan, Chemical mechanical planarization of copper in alkaline slurry with uric acid as inhibitor, Electrochim. Acta, 52 (2007) 6353-6358.

[24] M.C. Turk, M.J. Walters, D. Roy, Experimental considerations for using electrochemical impedance spectroscopy to study chemical mechanical planarization systems, Electrochim. Acta, 224 (2017) 355-368.

[25] F. Gao, H. Liang, Material removal mechanisms in electrochemical-mechanical polishing of tantalum, Electrochim. Acta, 54 (2009) 6808-6815.

[26] M.A. Amin, S.S. Abd El-Rehim, E.E.F. El-Sherbini, R.S. Bayoumi, The inhibition of low carbon steel corrosion in hydrochloric acid solutions by succinic acid, Electrochim. Acta, 52 (2007) 3588-3600.

[27] W. Liu, D. Wang, X. Chen, C. Wang, H. Liu, Recurrence plot-based dynamic analysis on electrochemical noise of the evolutive corrosion process, Corros. Sci., 124 (2017) 93-102.

[28] S. Caines, F. Khan, Y. Zhang, J. Shirokoff, Simplified electrochemical potential noise method to predict corrosion and corrosion rate, Journal of Loss Prevention in the Process Industries, 47 (2017) 72-84.

[29] X. Liu, T. Zhang, Y. Shao, G. Meng, F. Wang, In-situ study of the formation process of stannate conversion coatings on AZ91D magnesium alloy using electrochemical noise, Corros. Sci., 52 (2010) 892-900.

[30] P.-Q. Wu, J.P. Celis, Electrochemical noise measurements on stainless steel during corrosion–wear in sliding contacts, Wear, 256 (2004) 480-490.

[31] W. Lu, J. Zhang, F. Kaufman, A.C. Hillier, A Combined Triboelectrochemical QCM for Studies of the CMP of Copper, J. Electrochem. Soc., 152 (2005) B17.

[32] B.-J. Cho, S. Shima, S. Hamada, J.-G. Park, Investigation of cu-BTA complex formation during Cu chemical mechanical planarization process, Appl. Surf. Sci., 384 (2016) 505-510.

[33] M. Nagar, D. Starosvetsky, J. Vaes, Y. Ein-Eli, Potassium sorbate as an inhibitor in copper chemical mechanical planarization slurry. Part I. Elucidating slurry chemistry, Electrochim. Acta, 55 (2010) 3560-3571.

[34] U. Bertocci, F. Huet, R.P. Nogueira, P. Rousseau, Drift Removal Procedures in the Analysis of Electrochemical Noise, CORROSION, 58 (2002) 337-347.

1) An integrated electrochemical method was used to analyze Cu-CMP slurry

2) PVP was found to be an alternative inhibitor

3) Modified equivalent circuit modes were established for PVP and BTA film on Cu

4) Physical absorption mode was specified for PVP inhibitor film